

Review

Fluoride glasses

JACQUES LUCAS

*Université de Rennes, Campus de Beaulieu, Laboratoire de Chimie Minérale D,
Unité Associée au CNRS no. 254, Avenue du Général Leclerc, 35042 Rennes,
France*

A new family of vitreous materials based on the glass forming ability of some specific fluorides is presented. Conditions of formation, stability against devitrification, chemical durability, and structural models are examined in comparison with the traditional oxide glasses. The ZrF_4 -based glasses and some other multicomponent materials are examined in depth in view of their promising optical properties, which arise from their broad transmission range from ultraviolet to mid infrared and their potential as ultratransparent materials for long distance repeaterless optical fibre. Other active optical applications of doped glasses, such as lasers and their electrical and magnetic properties, are also discussed.

1. Introduction

The term fluoride glasses (FG) refers to particular vitreous materials belonging to the general family of halide glasses in which the anions are from elements in group VII of the Periodic Table, namely fluorine, chlorine, bromine, iodine. In contrast to oxide-containing glasses and particularly silicates, which exist as natural minerals and occupy a dominating position in glass science, vitreous materials based entirely on inorganic halides are purely synthetic and their development started only in the middle of the seventies.

Before 1975, only a few halide systems [1] had been proved to be in glasses form and the interest in these miscellaneous glasses was purely academic. Two halide compounds were known to give viscous melts when heated, leading to easy glass formation upon cooling: these two halides were BeF_2 and $ZnCl_2$. Curiously, those two glasses have almost the same structure and are isotopic with SiO_2 -based glasses; the three-dimensional aperiodic framework is in the three cases based on corner-sharing tetrahedra which are, respectively, BeF_4 , $ZnCl_4$ and SiO_4 .

The glass-forming properties of BeF_2 have been known for over 50 years and by virtue of their low linear and non-linear indices of refraction and low dispersion [2], the so-called fluoroberyllate glasses are currently of interest as passive components for high energy lasers. However, the development of such glasses is limited by the extreme toxicity and hygroscopicity of BeF_2 -based materials despite the remarkable stability of the glasses against devitrification.

In the chloride family, the only compound which is able to lead to a vitreous material when melted and cooled without any combination with another chloride is $ZnCl_2$. Despite the optical interest of such glasses due essentially to their large domain of transmission lying from the ultraviolet to the $12\ \mu m$ region in the

infrared, the technological development of $ZnCl_2$ -based glasses has been prevented by their very great hygroscopicity.

The AlF_3 -based multicomponent glasses, which have been described by Sun in the fifties [3], require a rapid quench from the melt and their tendency to devitrify limits their potential interest as optical materials.

A significant step forward occurred in 1974 at the University of Rennes, when the author's group [4] discovered the glass-forming properties of ZrF_4 . The fluorozirconate glasses, in which the primary constituent was ZrF_4 , greater than 50 mol %, and BaF_2 the principal modifier, about 30 mol %, with additional fluorides such as ThF_4 , LnF_3 ($Ln =$ lanthanides) appear to be very promising materials for mid-infrared applications.

Subsequently, many other families of fluoride glasses have been discovered essentially in France: the transition metal fluoride-based group developed at the University of Le Mans [5] and the so-called heavy metal fluoride glasses (HMFG) based on thorium, rare earth, indium, zinc, barium fluorides, again discovered in Rennes [6]. These zirconium-free fluoride glasses, which appear to be the second generation of halide glasses for optical applications, are of special interest because of their larger transmission range especially in the infrared region, the infrared cut-off being located near $8\ \mu m$.

Infrared transmitting and multispectral glasses are of interest as materials for a broad range of components such as laser windows, infrared domes, lenses, filters, laser hosts. However, the most exciting properties of these new glassy materials are their potential ultratransparency, about hundred times better than the silicate-based glasses, and their promising applications in mid-infrared fibre optics including ultralong repeaterless links for telecommunications, power

transmission and sensor systems. This aspect of fluoride glass technology has been reviewed by Miyashita and Manabe [7], Tran *et al.* [8] and France *et al.* [9].

The optical properties of fluoride glasses in bulk samples, and especially the potential of infrared fibre preparation, have been intensively examined in many laboratories throughout the world, principally in the United States, Japan, Great Britain and France. The concerted efforts during the last decades have been such that, in a few years, the transparency of these fluorozirconate glasses has been lowered from thousands of dB km^{-1} to 0.7 dB km^{-1} , the best value claimed in February 1986 at $2.55 \mu\text{m}$ wavelength. This value is still far from the intrinsic theoretical loss estimated around $10^{-2} \text{ dB km}^{-1}$, but is a very good indication of the evolution of this very fast-growing field.

In addition, significant results have been obtained in the optical characterization of bulk fluoride glass samples. Among them, low refractive index and dispersion, low Rayleigh scattering, high threshold for laser damage, new matrix for lasers operating in the mid-infrared, are the most important.

A complete review of the field by Drexhage [10] and a tutorial article by Moynihan [11] give an excellent overview of this new domain of material science.

Four international symposia on halide glass science and engineering have been held over the period 1982 to 1987, the proceedings of the last two of which have been or soon will be published [12, 13].

2. Glass formation in fluoride chemistry

2.1. Inorganic fluoride materials; from NaF to UF_6

With its specific electronic structure $1s_2, 2s_2, 2p_5$, the fluorine atom is the most electronegative element of the Periodic Table and consequently it has a great tendency to attract one electron to take the stable Neon s_2p_6 structure. This saturation of the outer electronic shell is achieved either by transferring one electron from an electropositive atom, or by sharing common electrons.

In the case of metallic fluorides, MF_n , the nature of the chemical bond will essentially depend on the charge and the size of M. Sodium fluoride, NaF, for instance, is a pure ionic material with a stability which is essentially governed by coulombic forces. At high temperature, it will give a melt formed by isolated Na^+

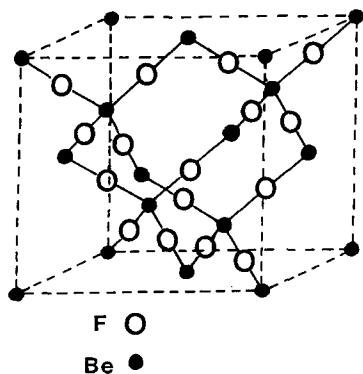


Figure 1 The SiO_2 cubic cristoballite structure, the parent crystalline model for BeF_2 fluoroberyllate glasses.

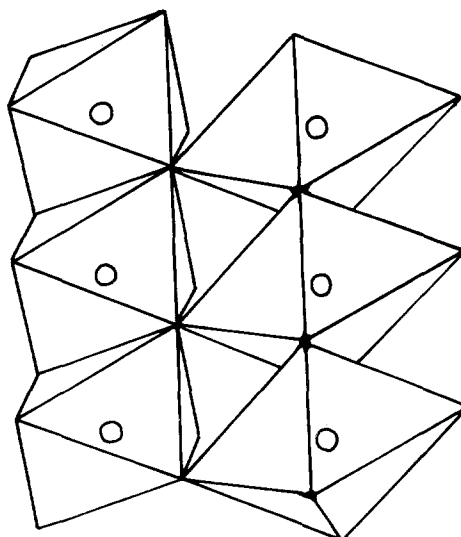


Figure 2 The rutile-type structure of divalent fluorides such as ZnF_2 . The ZnF_6 octahedra share corners and edges.

and F^- . These ions have a poor association and high mobility such that when cooling the solid obtained is purely crystalline.

The MF_2 family represented by BeF_2 , ZnF_2 and BaF_2 is the most interesting group showing for the same chemical formula a pure ionic compound BaF_2 in which F^- is coordinated by 4 Ba^{2+} and a highly covalent material BeF_2 due to the very high ionization potential of beryllium and in which fluorine is only surrounded by two beryllium atoms in a pure colinear sp hybridization.

This situation corresponds to the formation, by corner-sharing tetrahedra, of a giant three-dimensional covalent framework which belongs to the SiO_2 cristoballite type described in Fig. 1.

In ZnF_2 , which belongs to the TiO_2 rutile structure type, the zinc atoms are octahedrally coordinated and fluorine has a three-fold sp_2 coordination. The situation is here somewhat intermediate and the lattice is built up from ZnF_6 octahedra sharing edges and corners as indicated in Fig. 2.

The MF_3 family, represented by fluorides such as AlF_3 , FeF_3 , $\text{CrF}_3 \dots$, has a very simple structure in which M is octahedrally coordinated and F is surrounded only by two M atoms. This very open framework, made of octahedra sharing corners as indicated in Fig. 3, can be easily distorted by tilting the elementary modules.

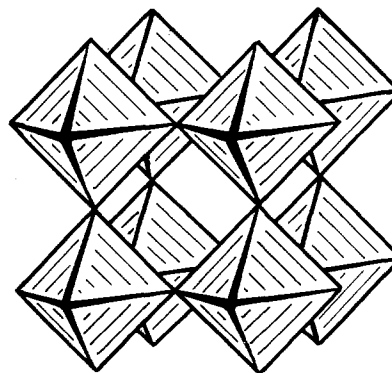


Figure 3 The three-dimensional framework of the MF_3 fluoride obtained by MF_6 octahedra corner sharing.

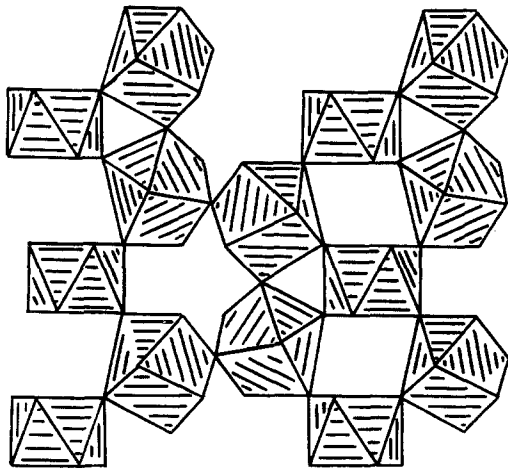


Figure 4 The ZrF_8 structure originating from elementary ZrF_8 polyhedra (distorted square antiprism) sharing corners in three directions.

The three fluorides ZrF_4 , UF_4 , ThF_4 are isotypic, and in their low temperature forms, their structure can be described as a three-dimensional network of MF_8 polyhedra sharing corners. The fluoride atoms are here also two-fold coordinated as shown in Fig. 4.

All the MF , MF_2 , MF_3 , MF_4 materials described are used for glass preparation; some of them play the role of glass former, being able to generate a three-dimensional framework, the others like BaF_2 , NaF , are more ionic, and play the role of lattice modifier.

If one examines the special case of fluoride materials containing small ions like Si^{4+} , Nb^{5+} , U^{6+} , which satisfy their own coordination without needing to share fluorine atoms, they form isolated molecules such as SiF_4 , Nb_2F_{10} , UF_6 , which tend to escape from the melt as volatile materials. The consequence is that, when one tries to introduce in a fluoride melt, at high temperature, materials containing Si^{IV} , even Ti^{IV} , Nb^V , U^{VI} , there is an immediate formation of fumes due to the high volatility of these molecular fluorides.

2.2. The glass-crystal competition in fluoride systems

As discussed previously, the first challenge for achieving glass preparation is the formation of a three-dimensional covalent framework halfway between pure ionic and pure molecular. However, this network during the cooling process from the liquidus to the solidus, must keep the isotropy and the aperiodicity of the melt.

There is, during this step, an obvious competition between keeping the disordered state of the liquidus and reorganizing the material in elementary unit cells, which in multiplying will lead to microcrystal formation, nucleation and then to the entire crystallization of the melt.

It is clear that the two thermodynamic factors competing during these phenomena are the diffusion kinetics of the different ions in the melt and the cooling rate.

If the melt contains large polymerized anions consisting in this case of MF_6 , MF_7 , MF_8 , MF_9 polyhedra sharing corners and edges, it is obvious that the viscosity will increase and that the diffusion of individual

ions to form elementary unit cells will be slow. This "confusion" in the melt is especially important when it contains Zr^{4+} and F^- . Indeed it is well known from examination of fluorozirconate chemistry, that the number and the variety of ZrF_n polyhedra are unique in crystal chemistry: with $n = 6, 7, 8, 9$, more than ten ideal coordination types have been described.

In all the cases, the tendency to form giant anions by corner or edge sharing is essential. The glass chemists involved in fluoride glass research know that the tendency towards crystallization of fluoride melts is very great and that rapid quenching is necessary to obtain glasses, when the melt is fluid. On the other hand, when, by suitable modification of the glass composition, the viscosity of the melt increases, the critical region from liquidus to solidus can be crossed with moderate cooling rates, which leads to glassy materials having a low tendency to devitrify.

2.3. The different families of fluoride glasses: a classification based on structural considerations

As previously discussed, conditions of glass formation are realized with materials having a chemical composition roughly situated between MF_2 and MF_4 ; the goal being the formation of a three-dimensional aperiodic network. Consequently, the fluoride glasses could be classified by reference to the elementary unit of their framework.

2.3.1. The MF_2 based glasses

These glasses are only represented by the BeF_2 glass family which shows a strong stability towards devitrification. According to Baldwin *et al.* [1], a general agreement exists to describe those vitreous materials as being isotypic of SiO_2 -based glasses. X-rays, molecular dynamics, etc, indicate clearly that the elementary unit is a BeF_4 tetrahedron and that the framework shown in Fig. 1 could lose its periodic character in bending and rotating the tetrahedra. The beryllium fluoride is the only fluoride material which easily vitrifies without adding any extra modifier cation. It must be noted that, when BeF_2 is associated with other fluorides such as KF , the glass obtained contains two kinds of fluorine: the bridging $Be-F-Be$ and the non-bridging $Be-F \dots K^+$.

Because of the high toxicity of beryllium and the hygroscopicity of many glass compositions, these glasses have not received much attention, except for some specific applications such as laser host for high-power delivery. These glasses are low melting materials with T_g in the vicinity of $350^\circ C$ and a liquidus temperature about $550^\circ C$.

2.3.2. The MF_3 -based glasses

These glasses, also called transition metal fluoride glasses, result from the formation of an aperiodic lattice due to MF_6 octahedra sharing corners. The MF_3 materials, which have been proved to give glasses when combined with appropriate other fluorides are AlF_3 , FeF_3 , CrF_3 , GaF_3 . Most of these investigations have been performed by Sun [3] and at the University of Le Mans, where they demonstrated that, for glass

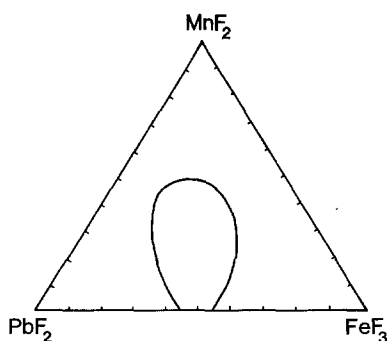


Figure 5 Vitreous domain in the ternary system $\text{FeF}_3\text{-MnF}_2\text{-PbF}_2$.

formation, these MF_3 fluorides have to be combined with divalent MF_2 such as ZnF_2 or MnF_2 and a modifier fluoride which is generally PbF_2 . As a good example, one can select the glasses of the ternary systems $\text{FeF}_3\text{-MnF}_2\text{-PbF}_2$, which is represented in Fig. 5. The glass composition PbFeMnF_7 , which is included in the vitreous domain, corresponds to a glassy material extremely rich in magnetic cations exhibiting interesting spin-glass properties at low temperature.

In this MF_3 -based group, the glass temperatures are in the range 300 to 400°C, crystallization occurs around 450°C and the liquidus is about 650°C. Most of these glasses have a great tendency to devitrify and this phenomenon is accelerated due to the sensitivity of these materials to moisture. Up to now, only a little information has been published on structural investigations of these glasses. From private discussions with the researchers of the University of Le Mans, it turned out that the most important results are as follows.

1. From X-ray scattering and EXAFS investigations, it appears that the M-F distances in most of these glasses are around 0.19 to 0.200 nm, which is consistent with the observed values in the parent crystalline compounds. The coordination number of F around M is six and the octahedron MF_6 is, as expected, the basic unit in these glasses.

2. From neutron, X-ray and modelling, it is obvious that the M-M distances are not exactly $\text{M-F} \times 2$. An average value of the M...M distance is about 0.38 nm indicating that the M-F-M is not colinear and that the octahedra due to rotation and bending are slightly tilted.

3. When PbF_2 is used for stabilizing the glasses, it is clear that the Pb^{2+} environment is typically consistent with its role of modifier.

The Fig. 3 could be used for modelling these glasses; the lack of periodicity is introduced by rotation and tilting of the octahedra and increased by the introduction of Pb^{2+} cations which from site to site, break the regularity of the network in generating non-bridging fluorine.

2.3.3. The ZrF_4 based glasses

These glasses have been at the origin of the development of this new class of materials. Although ZrF_4 by itself is not able to give a glass, if it is combined with a modifier fluoride such as BaF_2 , it leads to simple binary glass when fast quenching is used. As indicated in Fig. 6, the stability of the glasses towards devitri-

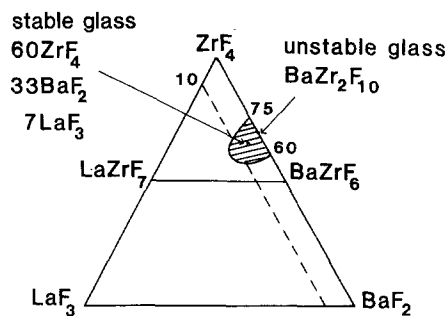


Figure 6 Glass formation area in a ZrF_4 ternary diagram. Here, ZrF_4 is associated with BaF_2 to form glasses which are more stable by addition of LaF_3 .

fication is strongly improved by using a third fluoride like ThF_4 or LaF_3 . The Fig. 6 represents the vitreous area in the diagram $\text{ZrF}_4\text{-BaF}_2\text{-LaF}_3$; the glasses having the lowest tendency to devitrify are located in the middle of the glassy domain. The rate of crystallization can also be decreased very significantly by using a small amount of AlF_3 . For instance, an optimized composition giving a good glass called ZBLA is 56 ZrF_4 , 34 BaF_2 , 6 LaF_3 , 4 AlF_3 .

The fluorozirconate glasses occupy a special position in this classification due to the extreme originality of the stereochemistry of the ZrF_n polyhedra. Examination of the general crystal chemistry of ZrF_4 -based materials indicates a great variety of polyhedra such as ZrF_6 , ZrF_7 , ZrF_8 and a unique diversity in the geometry of each of them. In addition, the tendency to polymerize by sharing corners or edges is also obvious and this gives a great flexibility in the Zr-F-Zr bonds. The result is the formation, in molten fluorozirconates of a confused situation due to the multiplicity of coordinations and consequently it appears difficult to generate a simple unit cell when cooling such a melt.

As discussed later, the basic units in these glasses are ZrF_7 and ZrF_8 polyhedra and more precisely the edge-sharing dimer Zr_2F_{13} which, by corner sharing, generates the three-dimensional aperiodic framework.

2.3.4. The multicomponent heavy metal fluoride glasses

It is possible to prepare heavy metal fluoride glass not containing zirconium [14] but the conditions of glass formation are more severe and at least three component compositions are necessary. In these glassy materials, the so-called "confusion" is introduced by multiplying the number of cations having, if possible, their own flexibility and variety in coordination number. Some examples of three-, four- and five-component glasses will be described and discussed as a function of their stability towards crystallization.

2.3.4.1. Three-component glasses. Fluoride glasses have been isolated in the following ternary systems, selected as typical examples: $\text{BaF}_2\text{-ZnF}_2\text{-LnF}_3$ ($\text{Ln} = \text{Y} \rightarrow \text{Lu}$); $\text{BaF}_2\text{-ZnF}_2\text{-ThF}_4$; $\text{BaF}_2\text{-ZnF}_2\text{-CdF}_2$; $\text{YbF}_3\text{-ZnF}_2\text{-ThF}_4$. In these examples, ZnF_2 can be partially or totally replaced by MnF_2 . The fluoride BaF_2 plays the role of modifier except in the last example which obviously contains only the network former cations Yb^{3+} , Zn^{2+} and Th^{4+} .

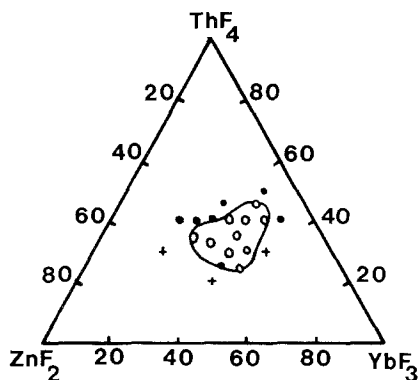


Figure 7 Vitreous domain in the ternary system $\text{YbF}_3\text{-ZnF}_2\text{-ThF}_4$. Severe quenching is necessary to obtain pure glassy materials.

The glassy area for this composition is indicated in Fig. 7 representing the $\text{YbF}_3\text{-ZnF}_2\text{-ThF}_4$ system. In all these examples, fast quenching is necessary to stabilize the glassy state and the small vitreous chips obtained have no practical interest. As an illustration of the high tendency to devitrify, these glasses have a $\Delta T_c - T_g$ in the range 50 to 60°C.

2.3.4.2. Four-component glasses. Systematic investigations of the quaternary diagram $\text{YbF}_3\text{-ThF}_4\text{-ZnF}_2\text{-BaF}_2$ indicate that when BaF_2 is added to the composition YbThZnF_9 , the critical difference $\Delta T_c - T_g$ increases, reaching a maximum value around 100°C for about 16% BaF_2 , as shown in Fig. 8.

Consequently, the optimized glass 16 BaF_2 , 28 ThF_4 , 28 YbF_3 , 28 ZnF_2 (BTYbZ), has a rather low tendency to crystallize and could be obtained as samples 1 cm thick. The ytterbium fluoride can be replaced by the neighbouring rare earth such as Lu^{3+} but not by the large lanthanides such as La^{3+} .

The relation between the confusion principle and the stability of the glass have also been verified in other four-component systems such as $\text{BaF}_2\text{-InF}_3\text{-ZnF}_2\text{-ThF}_4$. In this system, the glass showing the lowest tendency towards crystallization has the composition: 30 BaF_2 , 30 InF_3 , 30 ZnF_2 , 10 ThF_4 . In this case also, the value $\Delta T_c - T_g$ is about 100°C and samples of 1 cm are easily obtained.

2.3.4.3. Five-component glasses. To verify that the multiplication of cations having a flexible coordination was a good factor for increasing the confusion in the melt, and consequently decreasing the devitrification rate, a systematic investigation of the fluoride system $\text{Ba}_{30}\text{In}_{30}\text{Zn}_{30-x}\text{Yb}_x\text{Th}_{10}$ has been made.

For $x = 10$, the difference $\Delta T_c - T_g = 123^\circ\text{C}$ corresponds to the maximum value ever obtained for zirconium-free fluoride glasses, and samples 2 cm thick have been prepared. The liquidus temperature, $T_l = 650^\circ\text{C}$, for this fluoride glass, called BIZYbT ($\text{Ba}_{30}\text{In}_{30}\text{Zn}_{20}\text{Yb}_{10}\text{Th}_{10}$), is quite low when compared to the melting point of the single components: BaF_2 1355°C, InF_3 1170°C, ZnF_2 872°C, YbF_3 1157°C, ThF_4 1110°C. This shows clearly that the best glass compositions are in the vicinity of deep eutectic points in order to obtain a liquidus in which the thermal agitation is minimum for keeping the highest degree of polymerization.

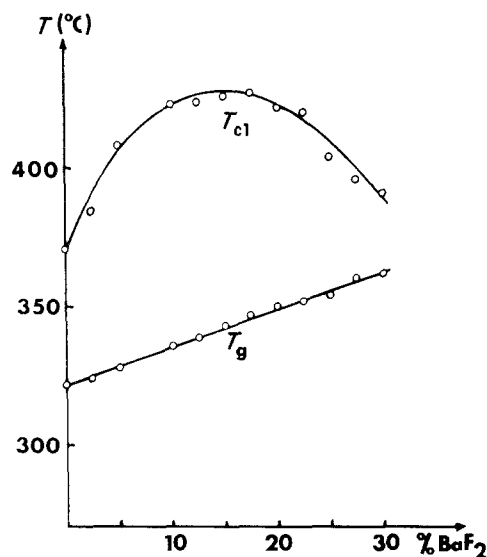


Figure 8 Evolution of $\Delta T_c - T_g$ as a function of BaF_2 addition to the ternary glass ThYZnF_9 . T_c is the first crystallization temperature. T_g is the glass temperature. The most stable glass against devitrification is obtained for $\approx 16\%$ BaF_2 .

2.4. Structural investigations on heavy metal fluoride glasses

Although the structure of vitreous materials cannot be determined unambiguously, the convergence of various and complementary methods increases the probability of being close to a model which will fit the observed physical properties, such as thermodynamic, spectroscopic, electrical, etc.

This brief review will give, without deep critical discussion, the most probable models describing the ZrF_4 -based glasses.

By nature, the multicomponent glasses cannot be modelled easily due to the high number of pair interactions. Therefore, it seems obvious that the zirconium-free glasses have a strong analogy with the fluorozirconates in the sense that the richness of ZrF_n polyhedra is replaced in the multicomponent materials by a variety of different MF_n groups.

The data used for these descriptions originate from global methods such as X-ray scattering, neutron scattering, molecular dynamics or methods such as spectroscopy using local probes. In this latter case, the tendency to generalize from partial information could lead to incorrect interpretation of the whole structure.

The binary system $\text{BaF}_2\text{-ZrF}_4$ provides the most simple example of fluorozirconate glass; the glassy domain extends from 50% to 75% ZrF_4 and the most easy material to obtain by moderate quenching is the glass $\text{BaZr}_2\text{F}_{10}$. It contained only three atoms different by their coordination number, scattering factor, charge and size, and is a good prototype to investigate the vitreous structure of ZrF_4 -based materials.

The most important results are reported in [12], Phifer [39] and Lucas [15] and cover either the so-called global methods such as X-ray, neutron scattering, molecular dynamic, vibrational spectroscopy, and the "local probe" technique giving informations on the local environment.

2.4.1. Results from global methods

Examination of the radial distribution function

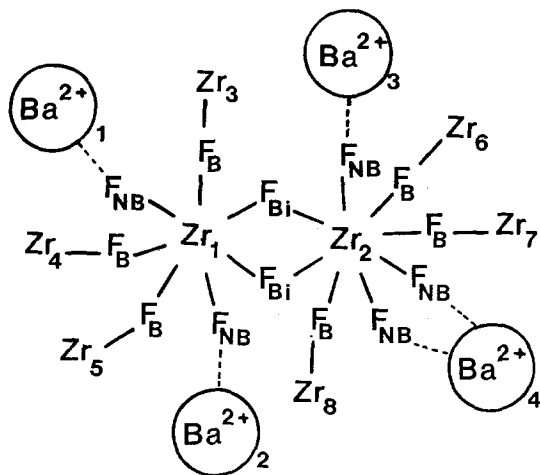


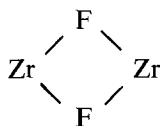
Figure 9 Formation of the elementary polyhedra Zr_2F_{13} by association edge-sharing of ZrF_7 and ZrF_8 . This bipolyhedron is interconnected with itself in the three-dimensional direction through the fluorine bridging. The other fluorine non-bridging atoms interact with the modifier Ba^{2+} cations.

(RDF) obtained either by X-ray or neutron scattering has been performed in comparison with the results originating from a quite different method called molecular dynamics which is based on the calculation of the minimum potentials using an electrostatic coulombic model. Both methods are in good agreement and lead to the following results.

(a) Zirconium, which is the key atom, is surrounded by fluorine atoms at a distance $Zr-F = 0.210$ nm. The coordination number (CN) is 7.5 indicating an almost equivalent distribution of ZrF_7 and ZrF_8 polyhedra; a few MF_6 and MF_9 coordination numbers are, of course, not excluded.

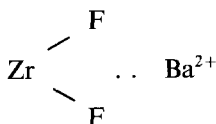
(b) Barium is surrounded by 11 fluorine atoms in a distribution of about 7.5 short $Ba-F$ and 3.5 long $Ba-F$.

(c) Examination of the $Zr-Zr$ pairs shows unambiguously the existence of a short $Zr-Zr$ distance of 0.360 nm due to



edge sharing and a long $Zr-Zr$ distance of 0.415 nm due to $Zr-F-Zr$ corner-sharing mechanisms.

(d) The $Zr \dots Ba^{2+}$ pairs in the 0.4 to 0.5 nm region can be interpreted as originating from $Zr-F \dots Ba^{2+}$ long interactions and



short interactions.

2.4.2. Results from local methods

Absorption and emission spectroscopy on rare earths (RE) such as Eu^{2+} , Eu^{3+} , Nd^{3+} , Er^{3+} , Ho^{3+} , Pr^{3+} and Mössbauer spectroscopy on Eu^{2+} and Eu^{3+} provide a useful tool to obtain information on the local structure [15]. All the results converge to imply that the RE

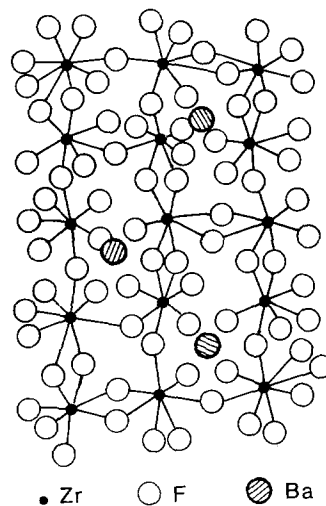


Figure 10 The three-dimensional aperiodic framework of the glass $BaZr_2F_{10}$. In this model the Ba^{2+} cations are statistically distributed in the Zr_2F_{10} negative framework originating from the polyhedra association described on Fig. 9.

environment is very well defined, as in a crystal, contrary to the situation in oxide glasses where the rare earths plays the role of modifier. It is concluded that, as expected, the RE ions are located inside the glassy network in a very precise coordination number estimated between 8 and 9 fluorine atoms depending on the lanthanide.

2.4.3. A structural model

The results briefly presented below lead to the conclusion that the elementary units in these glasses are ZrF_7 and ZrF_8 polyhedra and more precisely a binuclear polyhedron Zr_2F_{13} originating from corner sharing of the two previous ones, as indicated in Fig. 9. The three-dimensional aperiodic framework originates from corner-sharing of these elementary dimers as shown in Fig. 10.

The Ba^{2+} cations, due to their own repulsion, are randomly distributed in the aperiodic skeleton where they have strong ionic interactions mainly with the non-bridging fluorides.

3. Optical properties of fluoride glasses

3.1. Infrared transmission

Except for fluoroberyllate glasses which have their infrared cut-off located in the $4 \mu m$ region, the large transmission range lying from 0.2 to $8 \mu m$ is the most specific optical property. The infrared cut-off depends greatly on the chemical composition and is governed by the multiphonon absorption mechanisms which are related to the fundamental lattice vibrational modes.

The vibrational modes are, of course, related to the M-F chemical bond strength and it is observed that the multiphonon edge moves towards short wavelengths when small and strongly polarizing cations, such as Al^{3+} , are inserted in the glass. Fig. 11 shows the transmission range of fluoride glasses compared to silica-based glasses.

3.2. Refractive index and dispersion

The range of refractive index, n , of heavy metal fluoride glasses is 1.48 to 1.54 which is comparable to

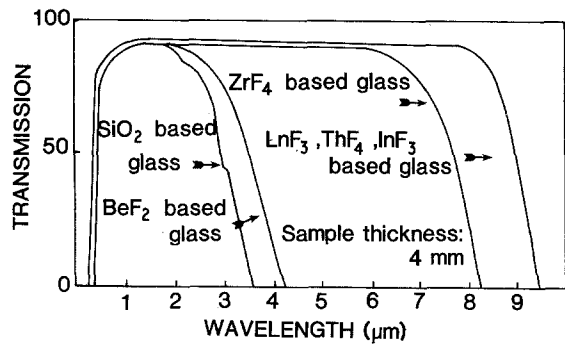


Figure 11 The optical transmission curve for SiO_2 glasses, BeF_2 glasses and two types of heavy metal fluoride glasses; one is ZrF_4 based, the other one is a multicomponent glass, for example InF_3 , based such as BIZYbT (see text).

the silica-based materials, but higher than the value observed for the BeF_2 -based glasses which are the glasses showing the lowest n value: 1.3 to 1.4.

The refractive index, n , can be easily tailored by changing the composition: light elements such as Li^+ or Al^{3+} decrease n while polarizable heavy elements, for instance Pb^{2+} , Bi^{3+} or even Cl^- , allow the preparation of glasses with a high index. Usually, doping has a poor effect on the stability of the glass towards devitrification and makes the design of a core-clad optical fibre with large n difference difficult to realize.

The Abbe numbers for most of the fluoride glasses are higher than those for oxide glasses. Values in the range 70 to 80 indicate that the variation of n with wavelength λ from 0.4 to $5\ \mu\text{m}$ is gentle and that the optical dispersion is weak which is an important factor for avoiding chromatic aberration in bulk optics.

A key quantity in optical fibre communication is the pulse broadening which is associated with the material dispersion which is proportional to $d^2n/d\lambda^2$. The zero material dispersion, for most of the fluoride glasses, is located around $1.7\ \mu\text{m}$ which is relatively far from the ultratransparency region close to $2.6\ \mu\text{m}$, as discussed in the next paragraph. Fortunately, the slope of the dispersion curve changes gently with λ and it has been demonstrated by France *et al.* [9] and Takahashi [16] that, in using a simple step-index design, the dispersion characteristics of the fibres can be tuned to give zero dispersion at the $2.55\ \mu\text{m}$ operating wavelength.

3.3. Potential of ultratransparency

When light passes through a material, two intrinsic mechanisms are responsible for total absorption losses:

(a) the scattering losses, called Rayleigh scattering, which follows a λ^{-4} law and consequently decreases rapidly with λ ;

(b) the multiphonon loss due to vibrational modes and which increases with λ . One must mention that the band gap absorption which is located in the ultraviolet for these materials does not play a significant role in the mid infrared.

The combination of both mechanisms gives the so-called V-shaped curve represented in Fig. 12 for SiO_2 and two families of fluoride glasses: a ZrF_4 -based material, ZBLA, and a multicomponent InF_3 -based glass, BIZYT.

The predicted lowest loss of $0.2\ \text{dB km}^{-1}$ at $1.55\ \mu\text{m}$

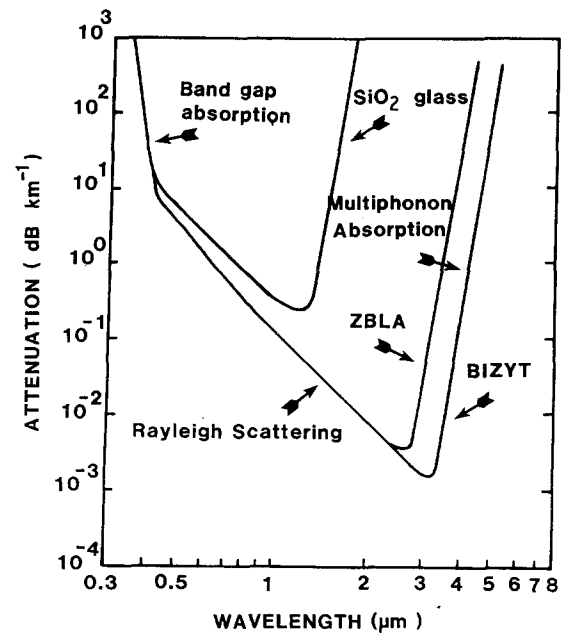


Figure 12 The V-shaped curve for SiO_2 and two fluoride glasses. (1) ZrF_4 glass called ZBLA. (2) A multicomponent based on indium and barium fluorides called BiZyBt (see text). The ultratransparency region is located between the two high absorbing zones due to bandgap plus Rayleigh scattering on one side and multiphonon absorption on the other side.

for silica has been reached by preparing optical fibre from ultrapure materials using chemical vapour deposition techniques.

The potential of fluoride glasses with expected loss as low as $0.01\ \text{dB km}^{-1}$ is extremely exciting, especially for long-distance communications such as undersea systems. Therefore, one must be aware that other factors of absorption, extrinsic in nature, will strongly affect the total transparency of fluoride glasses. Among them, scattering losses due to inhomogeneities, bubbles, microcrystals are the most important. In addition, parasitic species due to metallic impurities such as rare earth or transition metals and complex anions such as OH^- , SO_4^{2-} introduce severe absorption in the visible and mid infrared as indicated in Fig. 13.

3.4. Infrared transmitting fluoride glass optical fibres

As previously mentioned, the minimum level of attenuation around $0.2\ \text{dB km}^{-1}$ has been reached with silica fibres leading to effective telecommunications link of 50 to 100 km without repeater.

Fluoride glasses potentially offer intrinsic minimum losses one or two orders of magnitude lower than that of silica. As shown in Fig. 12, the estimated lowest value is in the range 10^{-2} to $10^{-3}\ \text{dB km}^{-1}$ and the ultralow loss optical window is located in the 2 to $4\ \mu\text{m}$ region. In fact, due to the difficulty of eliminating completely the transition metal and especially the OH impurities, it is obvious that the window will be narrow and located between these two absorption regions, namely between 2.5 and $2.6\ \mu\text{m}$.

A concerted research effort, conducted mainly by telecommunications people in the USA, Japan, UK, Germany and France, has gone into developing

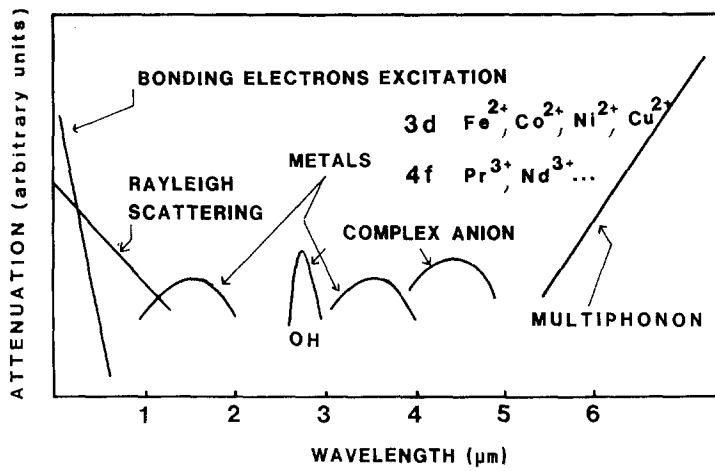


Figure 13 Extrinsic factors introducing parasitic absorption in fluoride glasses. Transition metals and rare earths are the most poisonous in the visible and near infrared while complex anions such as OH^- , SO_4^{2-} , etc., have their absorption in the mid infrared. The total attenuation can also be strongly affected by extrinsic scattering factors such as bubbles, cristallites.

appropriate glass compositions and fibre-pulling technology in order to reach this ultra-low loss level.

As discussed previously, in addition to intrinsic mechanisms, many extrinsic factors disturb the ultratransparency and the preparation of high-quality fluoride glasses with low absorption is a difficult challenge which requires the synthesis of ultrapure fluoride chemicals as discussed by Folweiler and Guenther [17].

Among the most poisonous cations absorbing in the $2.55 \mu\text{m}$ region, where the expected ultratransparent window is located, the transition metals Cu^{2+} and Fe^{2+} have the most dangerous effect and solvent extraction techniques are necessary in order to purify the starting materials. The rare-earth metals, and among them Nd^{3+} with an absorption peak at $2.5 \mu\text{m}$, also have to be reduced to the p.p.b. level in order to keep the expected ultratransparency.

Fluoride glasses are known to be prone to devitrification and fibre-making techniques have to take into account this important factor in order to avoid formation of microcrystallites which have a drastic effect on

scattering loss. Fig. 14 shows the different steps in the double index preform fabrication. In order to keep the light inside the optical waveguide when carrying the optical signals over very long distances, the core must have a refractive index slightly superior to that of the cladding. This is achieved by modifying the chemical composition of both glasses; typically a small amount of PbF_2 increases n while LiF does the inverse.

Present fluoride glass fibre technology relies strongly on the preform casting approach. In this approach, core melts are directly cast into cladding tubes to form waveguide preforms. Fluoride glass cladding tubes with uniform wall thickness can be obtained by rotational casting. The preforms are then drawn at around the glass softening point, $T \approx 350^\circ\text{C}$, in order to avoid crystallization. After drawing a preform of 10 mm diameter and 20 cm length, the usual fibre diameters are about $150 \mu\text{m}$. The preform approach leads necessarily to limited fibre lengths which will need the development of low-loss splicing techniques. In order to prepare ultralong fibres, a continuous fabrication process appears to be very attractive. As

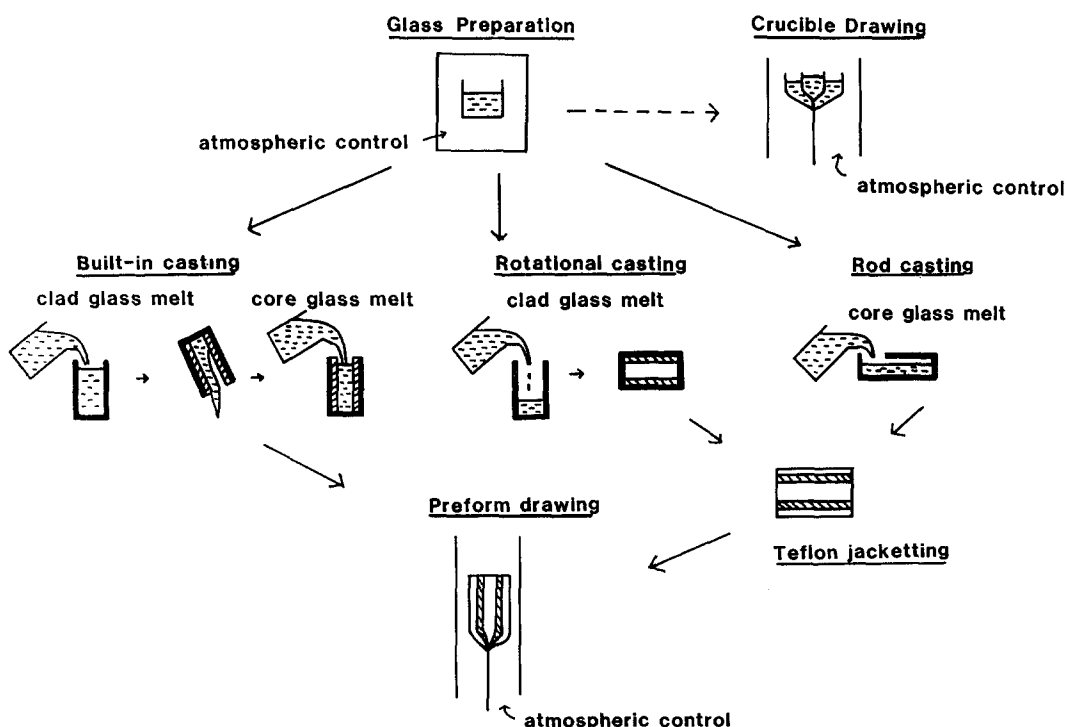


Figure 14 Technical routes for fluoride glass preform preparation and fibre drawing.

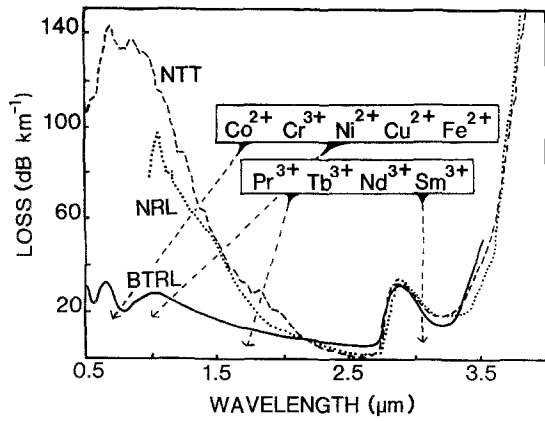


Figure 15 Infrared transmission curve for fluoride glass fibres originating from NTT, NRL and BTRL. This figure is adapted from France *et al.* [9].

shown in Fig. 14, the so-called double crucible technique, which is based on the direct preparation of two index fibres from two concentric melts, is in principle the most promising. However, the fluoride melts are known to have a very sharp viscosity-temperature dependence and the diameter control during fibre pulling needs a very severe stabilization of the melt temperatures.

The major efforts conducted either in Nippon Telegraph Telephone (NTT; Japan), Naval Research Laboratories (NRL; USA) and British Telecommunication Research Laboratories (BTRL; UK) have led to a continuous lowering in the absorption losses and values as low as 0.7 dB km^{-1} at $2.55 \mu\text{m}$ have been obtained by using traditional purification techniques. Fig. 15 represents typical transmission spectra for the best fluorozirconate glass fibres prepared either in England, Japan or USA. It must be noted that the BTRL transmission curve is flat over a large domain of wavelength and is given for a 200 m length with a minimum of about 3 dB km^{-1} . The NRL curve is for an unspecified length with a minimum of 0.9 dB km^{-1} and the NTT data correspond to the lowest value of 0.7 dB km^{-1} on a 30 m length fibre.

This representation summarizes the situation and indicates the key factors which must be optimized to improve the transparency of the waveguides. Among them, the OH peak at $2.9 \mu\text{m}$ is the most important and, with a value of about 30 dB km^{-1} , it corresponds to a very small content of OH evaluated at a few tens p.p.b. OH.

The transition metals, such as Fe^{2+} , Cu^{2+} , Co^{2+} , absorbing from 1 to $2 \mu\text{m}$, the rare-earth ions such as Nd^{3+} , Tb^{3+} , Sm^{3+} having their electronic transitions in the 2 to $3 \mu\text{m}$ region are the other factors responsible for the absorption background. In addition, scattering is also a severe cause of loss. One can estimate that scattering accounts for two-thirds of the total loss.

According to France *et al.* [9], a realistic total loss of 0.035 dB km^{-1} could be expected if the impurity level is assumed to be maintained in the range of 0.1 to 5 p.p.b. This loss corresponds to a capability of repeaterless information transmission over a distance of 1500 km.

Recent improvements of the surface of the glass by etching the preform rod have been proved to increase the strength of fibres and have been described recently by Schneider *et al.* [18].

Among the potential uses for fluoride glass (FG) optical fibres, the realization of very long repeaterless telecommunications links for undersea systems, for example, is the most challenging and will need additional research effort, especially in chemical purification. However, the actual level of transparency of FG optical fibres is such that these new waveguides can be used in many short length devices, for example, for remote sensing and thermal imaging out to about $5 \mu\text{m}$. Commercial devices include, for instance, the coupling between an Er^{3+} YAG laser emitting at $2.9 \mu\text{m}$ and an FG fibre for power delivery in surgical applications because water in tissues absorbs strongly at this wavelength. Gas lasers such as HF emitting at $2.6 \mu\text{m}$ and DF emitting at $3.8 \mu\text{m}$ can also be used as the power source. Low loss bulk optical components made in FG will be also very convenient for realising prisms and lenses, operating in the mid infrared as well as optical windows with a high damage threshold for high energy lasers such as HF.

3.5. Active optical devices

Transition metal and rare-earth fluorides can be easily dissolved and incorporated in FG and exhibit optical phenomena associated with the presence of partially filled 3d or 4f electronic shells. These coloured glasses could be investigated either by considering these ions as local probes for structural information, or for producing fluorescent light for laser applications for instance. As previously indicated in the section devoted to structure, the rare-earth ions are, in this new matrix, in a very specific ligand field indicating that the lanthanide ions play the role of glass former and give a spectroscopic response in absorption and fluorescence which is almost the same as in a crystal: see for instance, in fig. 16, the fluorescence peaks of an Nd^{3+} FG sample compared to the parent crystalline material NdZrF_7 . It appears that the bandwidth of the two main emission peaks in the vitreous host has about the same magnitude as the crystal field splitting of the terminal states in the unique crystallographic

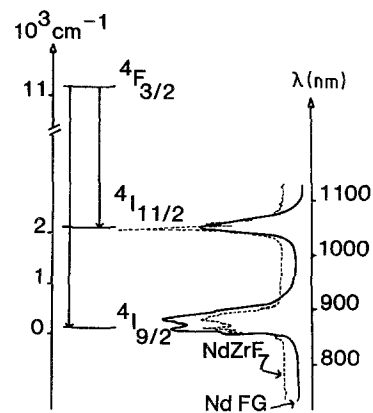


Figure 16 Emission fluorescence spectra of a Nd^{3+} -doped fluoride glass compared to the parent crystalline material NdZrF_7 . The envelope of the emission peak is almost the same in the crystal and in the glass.

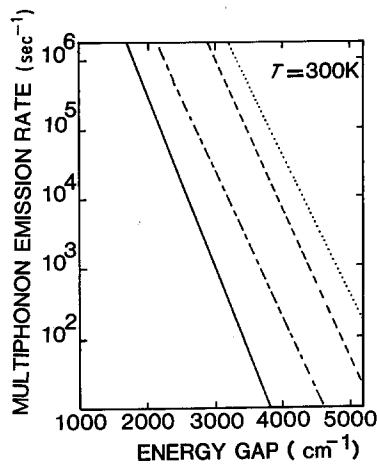


Figure 17 Multiphonon emission rates (or heat dissipation) plotted against energy gap for different glassy materials doped with rare-earths: ZBLA is a ZrF_4 -based glass. From Sibley *et al.* [19]. (—) ZBLA, (---) tellurite, (- - -) silicate, (···) phosphate.

site of $NdZrF_7$ crystal. The rare-earth emission peaks for the other rare-earths such as Eu^{3+} , Pr^{3+} , Ho^{3+} , . . . , have also been measured in FG and proved to be very narrow compared to other glassy matrices such as silicates, phosphates, and so on [15].

Sibley [19] and co-workers have examined the potential of fluoride glass for laser hosts and special attention has been paid by different authors [20, 21] to demonstrate the originality of the FG matrix for investigating the radiative rates as well as the oscillator strengths and branching ratio.

The lifetime of numerous transitions has been measured in order to determine the multiphonon emission rates and the energy-transfer rates and to compare these with the values obtained in other vitreous matrices such as silicates, phosphates, tellurite, etc. As a consequence, the potential for laser hosts and other active optical applications has been discussed by Sibley in referring to Fig. 17 which shows, for example, the multiphonon emission rate calculated at 300 K for different levels of Er^{3+} and Ho^{3+} as a function of energy gap. It is clear that energy loss by multiphonon emission, namely heat dissipation, is much more important in phosphate than in FG glass, in the range of several orders of magnitude for a given wavelength. Consequently, one can predict a high-emission efficiency of the rare-earth and because of the broad optical window of the host lying from 0.2 to $8\ \mu m$, an exceptional choice in the optical pumping and lasing wavelength.

According to Sibley *et al.* [22] and Quimby *et al.* [23], the fluoride glasses, and especially the multi-component zirconium-free materials, are excellent hosts for observing the conversion of infrared to visible light. This so-called up-conversion process or Auzel effect results from a photon addition mechanism involving energy transfer from Yb^{3+} ions excited around $1\ \mu m$ and playing the role of donor to Er^{3+} ions being the acceptor and converting two infrared photons in a green light with a $\lambda = 0.53\ \mu m$. Here also, the efficiency is remarkable around 2% compared to other glasses and allows visual detection even for low incident infrared light.

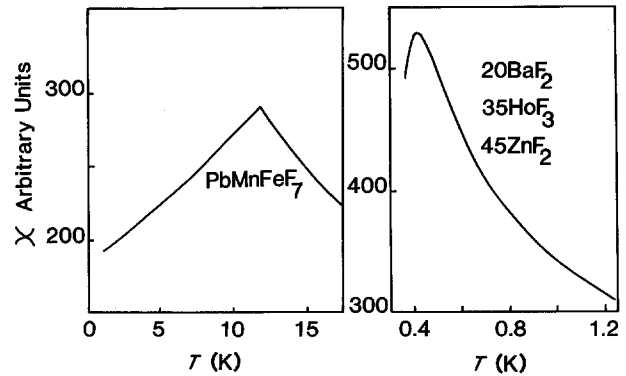


Figure 18 Evolution of the magnetic susceptibility with temperature for fluoride glasses containing (1) a large amount of transition metal (Mn^{2+} , Fe^{3+}), (2) high concentrations of Ho^{3+} . In both cases, a spin-glass behaviour with antiferromagnetic interactions is obvious at low temperature.

4. Magnetic and electrical properties of fluoride glasses

4.1. Magnetic behaviour of metallic-doped FG

Fluoride glasses offer unique opportunities to study the magnetic properties of amorphous disordered systems because they exhibit a large range of glass compositions, high atomic concentrations and various associations of magnetic ions belonging either to the 3d or 4f series. These properties have been essentially investigated by Dupas and co-workers [24, 25] on many FG compositions containing either high concentrations of magnetic lanthanides or 3d metals such as iron or a combination of both species. As an example, we shall select the glass $PbMnFeF_7$ belonging to the 3d metal system $PbF_2/MnF_2/FeF_3$ and a rare-earth-rich material with the composition $20BaF_2$, $35HoF_3$, $45ZnF_2$. Most of these magnetic glasses are usually unstable towards devitrification and need to be obtained by quenching.

The magnetic susceptibility of doped fluoride glasses follows a Curie-Weiss law over a wide range of temperature. These systems exhibit very low values of the Curie-Weiss temperature ($\theta \approx 100\ K$) evidencing antiferromagnetic interactions.

At low temperatures, as indicated in Fig. 18, a cusp occurs in the thermal variation of the a.c. susceptibility, indicating the onset of spin-glass ordering. The spin freezing temperature, $T_f > 10\ K$ is remarkably high for the glass $PbFeMnF_7$ containing large amounts of 3d⁵ cations Fe^{3+} and Mn^{2+} , compared to the Ho^{3+} containing glass where $T_f < 1\ K$.

Many investigations have been conducted on this type of magnetic material in order to see the effect of metallic substitutions on the properties and to clarify the nature of the spin-glass interactions in these insulating materials.

4.2. Electrical properties

Electrical investigations on fluoride glasses have been initiated by Ravaine and co-workers [26, 27]. They conclude that the main features of the electrical behaviour of this new vitreous materials were:

(a) as expected, they are very poor electronic

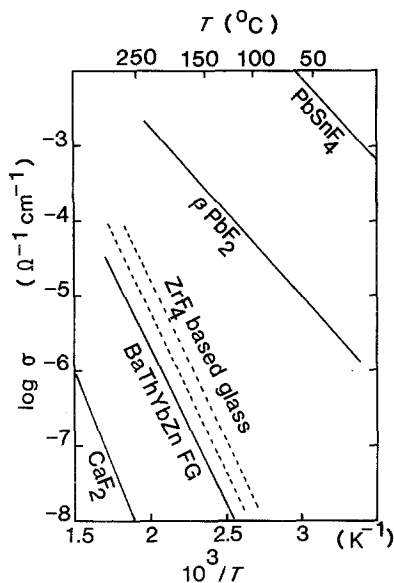


Figure 19 Conductivity of fluoride glasses plotted against temperature, compared to other fluoride solid electrolytes such as good conductors, namely PbSnF_4 , and a poor conductor, for instance CaF_2 . This figure is adapted from the work of Ravaine [26].

conductors taking into account the very electronegative character of the fluorine atoms;

(b) the conductivity measured on many samples and compositions is about $\sigma = 10^{-6} \Omega^{-1} \text{cm}^{-1}$ at 200°C .

(c) the conductivity mechanism is only due to F^- ion mobility which gives to these glasses solid electrolyte properties and makes them candidates for a solid state battery involving F_2 or derivatives at one electrode;

(d) the activation energy is very dependent on the composition and is in the range $E = 0.66$ to 0.89 eV .

Kawamoto and Nohara [28] confirmed these results and Inoue and Yasui [29] have proposed a conductivity mechanism from molecular dynamics simulations which shows that the dominant factor of the conduction is due to the migration of the non-bridging fluorine ions. The fluorine mobility can be explained by the plurality of the ZrF_n polyhedra ($n = 6, 7, 8$) in the glass, as discussed in the section on structure. This situation can be compared to the mixed valence effect in electronic semiconductors.

Fig. 19 shows the conductivity–temperature diagram for different crystalline and vitreous fluoride conductors. It appears that all the FG compositions are located in the same order of conductivity, approximately between the very good fluorine conductors such as PbSnF_4 and the poor fluorine conductors such as CaF_2 .

5. Chemical durability, devitrification, purification

5.1. Chemical durability

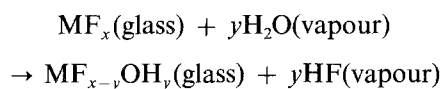
Fluoride glasses are strongly resistant to corroding agents such as F_2 , HF , UF_6 gases. In combining their optical transparency and good resistance to corrosion, they are ideal materials for photochemical reactors containing these aggressive reagents.

These materials are not hygroscopic and could stay in the normal laboratory atmosphere without any attack of the surface. Therefore, the water molecules,

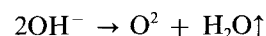
H_2O , react with fluoride glass and the corrosion mechanisms depend on the temperature and if the water is liquid or vapour.

When a piece of glass is immersed in water, the corrosion kinetics depends on the pH; in acidic conditions, the proton H^+ reacts rapidly with the F^- ions of the glass to form HF , the corresponding OH^- takes the place of the F^- in the structure; at the same time, the modifier cations such as Ba^{2+} , Na^+ diffuse into the solution. According to Simmons and Simmons [30], the total mechanism corresponds to a dissolution of the matrix with a very fast migration of certain species such as Li^+ , Na^+ , Al^{3+} into the solution. The direct consequence is that the ZrF_4 -based glasses have a chemical durability in non-basic solutions comparable to the poorest silicates. The direct result of these chemical modifications is the devitrification of the corroded surface which rapidly crystallizes and forms an opaque film on the surface. In basic solutions, the stability of the glass is much higher and some compositions could stay in these conditions for a few weeks without apparent corrosion.

The corrosion by H_2O vapour is quite different [31]; depending on the composition, it usually starts just below the glass temperature around 300°C . The mechanism of corrosion is illustrated by the following reaction



This attack becomes significant when the temperature increases and is visually easy to detect when a fluoride glass melt is treated in normal atmosphere due to the formation of white fumes. The result of this corrosion is the presence of a strong OH absorption peak at $2.9 \mu\text{m}$ in the glass and the potential formation of oxides playing the role of nucleation agents according to the reaction



By measuring the amount of HF produced in the pyrohydrolysis reaction, it is possible to establish the relation between the value of the OH^- peak and the proportion of OH as demonstrated by Fonteneau *et al.* [32] and Mitachi *et al.* [33]. From this observation, the molar extinction coefficient ϵ_{OH^-} at $2.9 \mu\text{m}$ has been calculated for various FG and consequently the attenuation loss introduced by 1 p.p.m. OH has been estimated; as an example, the attenuation β is a $7850 \text{ dB km}^{-1} \text{ p.p.m.}^{-1}$ for the BIZYbT glass and $5200 \text{ dB km}^{-1} \text{ p.p.m.}^{-1}$ for the ZBLA glass.

The practical effect of this corrosion phenomenon leading to hydroxyl, then oxide formation, is the risk of nucleation and crystallization originating from the surface and consequently the only way to prepare good optical glasses is to operate in a dry glove-box.

5.2. Devitrification

As discussed by Moynihan and co-workers [11, 34], one of the major problems encountered in the development of heavy metal fluoride glass has been the tendency for the glasses to devitrify above the glass transition temperature. Also, during the cooling

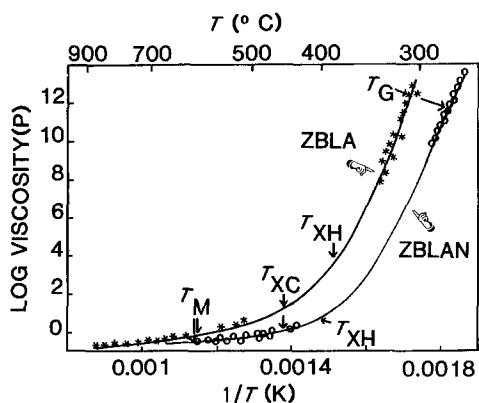


Figure 20 Viscosity plotted against temperature for two technical fluoride glasses ZBLA and ZBLAN. In both cases, the lack of data in the intermediate region is due to crystallization phenomena. The different temperatures are the following: T_G glass temperature; T_M liquidus; T_{XC} and T_{XH} = crystallization on cooling and heating.

process of the melt, there is a critical cooling rate to avoid the nucleation [35] of the melt and then the growth of the crystallites [36].

The main feature illustrating the special thermal behaviour of FG is the temperature dependence of the viscosity which is represented in Fig. 20. It is clear that there is a large gap between the high-temperature viscosity data collected in the melt by Mackenzie [37] and co-workers and the highly viscous zone just after T_g . This situation is due in part to the tendency of these melts to crystallize mainly because the viscosity is only a few poise at temperatures significantly below the liquidus allowing relatively high mobility of the ions for nucleation and crystallization processes.

Fig. 20 is a comparison of two good technical glasses: 1, ZBLA with the composition $Zr_{55}Ba_{35}La_6Al_4$; 2, ZBLAN with the composition $Zr_{55}Ba_{17}La_6Al_4Na_{18}$. The second has been proved to be more resistant to devitrification and is one of the best candidates for fibre drawing. This interesting behaviour is explained by an interdiffusion barrier to crystallization due to the competition between two crystalline forms. Indeed, it has been noticed that a partial substitution of the modifier cation Ba^{2+} by Na^+ cations introduces a competition between sodium fluorozirconate and barium fluorozirconate formation during the crystallization process and consequently delays the devitrification phenomena.

This observation appears to be a kind of illustration of the so-called confusion principle and could explain that one route to finding FG compositions more stable against crystallization may be to incorporate into the melt additional components which will inhibit the first crystalline species formation.

5.3. Purification

The conventional route for preparing fluoride glasses is the melting of the starting fluorides in an inert atmosphere using vitreous carbon, gold or platinum crucibles. The liquidus temperature for heavy metal fluoride glasses being around 550 to 650°C, moderate heating until 800 to 850°C is needed to obtain a homogeneous melt.

Another convenient way to prepare the melt is the

ammonium fluoride route using NH_4FHF which easily converts oxides in fluorides. The conversion reaction takes place at temperatures around 300 to 400°C and an excess of ammonium fluoride is needed to transform completely the oxides in a mixture of metallic ammonium fluorides which are then decomposed by heating at 800°C. This treatment eliminates the excess of NH_4FHF and produces a melt which is poured in preheated brass moulds. The glasses are then annealed at a temperature close to T_g .

As mentioned before, the development of high optical quality optics or optical fibres is governed by the production of high-purity materials where one must avoid the presence of transition metal, rare earth, complex anions such as OH^- , SO_4^{2-} , PO_4^{3-} , etc. which absorb in the optical window of fluoride glasses.

Sublimation of volatile fluorides such as ZrF_4 as well as solvent extractions are the most common techniques used for purifying the starting fluorides from the most poisonous absorbing cations such as Fe^{2+} , Cu^{2+} , Co^{2+} , Ni^{2+} , Nd^{3+} , Ce^{3+} , Pr^{3+} . It must be noted that 1 p.p.m. of these impurities leads to parasitic absorption in the range of 10 to 100 dB km⁻¹ and that the tolerated level of contamination for reaching the ultimate transparency values will have to be at the part per billions level.

Purification based on chemical vapour deposition also seems to be a solution for separating transition metals. The vapour pressure of $ZrCl_4$ and $ZrBr_4$ is, for instance, a few orders of magnitude higher than the transition metal equivalents. Their conversion in ZrF_4 through the vapour state via a fluorinating agent is an elegant way to produce very pure starting materials [17].

The natural impurity of fluoride material is OH^- due to hydrolysis with HF formation. In order to decrease the level of OH^- which introduces a large absorption band in the middle of the optical window, a "reactive atmosphere processing" (RAP) techniques has been developed initially by Robinson [38]. A gaseous atmosphere, such as CCl_4 , SF_6 , NF_3 , CS_2 , used above the melt helps the substitution of OH^- and O^{2-} impurities by Cl^- , S^{2-} , etc. An NF_3 atmosphere also maintains an oxidizing situation above the melt which allows iron impurities to be retained in the trivalent non-infrared absorbing Fe^{3+} state.

It must be noted that O^{2-} impurity in fluoride glasses has two effects: it modified the multiphonon absorption mechanisms by the formation of M-O vibrational modes which introduce shoulders in the multiphonon region; depending on the degree of contamination, O^{2-} could contribute to the formation of ZrO_2 crystallite particles having a high lattice energy and producing a very poor effect on the Rayleigh scattering factor even if the particles are of the 0.2 μm range size [16]. Using the RAP technique for decreasing the oxygen content in glasses is consequently justified especially for lowering the scattering loss mechanism in long-distance repeaterless optical fibre for telecommunication.

6. Conclusion

Heavy metal fluoride glasses, in addition to their pure academic interest as a new family of glasses, are

considered to be prime candidates for ultra-low loss fibre applications. Extensive purification efforts for the removal of transition metal, rare earth and OH groups have been conducted over recent years and it is considered that the ultratransparency window will be located between the metal absorption area around 1 to 2 μm and the OH peak at 2.9 μm . It is expected that further purifications of the raw fluoride materials, as well as a better knowledge of the fundamental properties and structure of these glasses, will lead to a new generation of ultra-low loss waveguides.

References

1. C. M. BALDWIN, R. M. ALMEIDA and J. D. MACKENZIE, *J. Non-Cryst. Solids* **43** (1981) 309.
2. M. J. WEBER, "Critical Materials Problems in Energy Production", edited by C. Stein (Academic, New York) (1976) pp. 267-79.
3. K. H. SUN, *J. Amer. Ceram. Soc.* **30** (1947) 277.
4. M. POULAIN and J. LUCAS, *Verres Réfract.* **32** (1978) 505.
5. C. JACOBONI, A. LE BAIL and R. DE PAPE, *Glass Tech.* **24** (3) (1983) 167.
6. J. LUCAS, H. SLIM and G. FONTENEAU, *J. Non-Cryst. Solids* **44** (1981) 31.
7. T. MIYASHITA and T. MANABE, *IEEE J. Quant. Electron.* **QE18**, (1982) 432.
8. D. C. TRAN, G. H. SIGEL and B. BENDOW, *J. Light-wave Technol.* **LT2** (1984) 566.
9. P. W. FRANCE, S. F. CARTER, M. W. MOORE and C. R. DAY, *Brit Telecom. Technol. J.* **5** (1987) 28.
10. M. G. DREXHAGE, in "Treatise on Materials Science and Technology", Vol. 26, edited by M. Tomozawa and R. H. Doremus (Academic, 1985) p. 151.
11. C. T. MOYNIHAN, *Mater. Res. Soc. Bull.*, to be published.
12. J. LUCAS and C. T. MOYNIHAN (eds) "Halide glasses", Vols I and II "Mater Science Forum", 5, 6 (Trans Tech., Aedermannsdorf, Switzerland, 1985).
13. M. G. DREXHAGE, C. T. MOYNIHAN and M. ROBINSON (eds) "Halide glasses", Vols III and IV, "Materials Science Forum", 19, 20 (Trans Tech., 1987).
14. J. LUCAS, in "Halide glasses for IR optics", edited by R. M. Almeida, NATO ASI series, Vol. 123 (Martinus Nijhoff, 1987) p. 321.
15. J. LUCAS, *J. Less Common Metals* **112** (1985) 27.
16. S. TAKAHASHI, *J. Non-Cryst. Solids* **95-96** (1987) 95.
17. L. C. FOLWEILER and D. E. GUENTHER, in "Materials Science Forum", 5, edited by J. Lucas and C. T. Moynihan (Trans Tech., 1985) p. 43.
18. H. W. SCHNEIDER, A. SCHOBERT, A. STAND and CH. GERDNT, *SPIE* **779** (1987) 112.
19. W. A. SIBLEY, in "Materials Science Forum", 5, edited by J. Lucas and C. T. Moynihan, (Trans Tech., 1985) p. 611.
20. R. REISFELD, E. GREENBERG, R. N. BROWN, M. G. DREXHAGE and C. K. JORGENSEN, *Chem. Phys. Lett.* **95** (1983) 91.
21. J. LUCAS, M. CHANTHANASINH, M. POULAIN, P. BRUN, M. J. WEBER, *J. Non-Cryst. Solids* **27** (1978) 273.
22. W. A. SIBLEY, D. C. YEH, M. SUSCAVAGE and M. G. DREXHAGE in "Materials Science Forum", 19, 20 (Trans Tech., Aedermannsdorf, Switzerland, 1987) p. 567.
23. R. S. QUIMBY, M. G. DREXHAGE and M. J. SUSCAVAGE, *ibid.*, 6, (1987) p. 557.
24. C. DUPAS, J. P. RENARD, G. FONTENEAU and J. LUCAS, *J. Magn. Magn. Mater.* **27** (1982) 152.
25. J. P. RENARD, C. DUPAS, E. VELU, C. JACOBONI, G. FONTENEAU and J. LUCAS, *Physica* **108B** (1981) 1291.
26. D. RAVAINÉ, "Materials Science Forum", 6 (Trans Tech., Aedermannsdorf, Switzerland, 1985) p. 761.
27. D. LEROY, J. LUCAS, M. POULAIN and D. RAVAINÉ, *Mater Res. Bull.* **13** (1978) 1125.
28. Y. KAWAMOTO and I. NOHARA, in "Materials Science Forum", 6, (Trans Tech. 1985) p. 767.
29. H. INOUE and I. YASUI, *ibid.*, 19, 20 (1987) p. 161.
30. C. J. SIMMONS and J. H. SIMMONS, *J. Amer. Ceram. Soc.* **69** (1986) 661.
31. S. R. LOEHR, K. H. CHUNG, C. T. MOYNIHAN, G. FONTENEAU, P. CHRISTENSEN and J. LUCAS, in "Materials Science Forum", 19, 20 (Trans Tech., Aedermannsdorf, Switzerland, 1987) p. 327.
32. G. FONTENEAU, D. TRÉGOAT and J. LUCAS, *Mater. Res. Bull.* **20** (1985) 1047.
33. S. MITACHI, G. FONTENEAU, P. S. CHRISTENSEN and J. LUCAS, *J. Non-Cryst. Solids* **92** (2-3) (1987) 326.
34. S. N. CHRIGHTON, R. MOSSADEGH, C. T. MOYNIHAN, P. K. GUPTA and M. G. DREXHAGE, in "Materials Science Forum", 19, 20 (Trans Tech., Aedermannsdorf, Switzerland, 1987) p. 435.
35. M. A. ESNAULT-GROSEMOUGE, M. MATECKI and M. POULAIN, *ibid.*, 5, (Trans. Tech., Aedermannsdorf, Switzerland, 1985) p. 241.
36. N. P. BANSAL, R. H. DOREMUS, C. T. MOYNIHAN and A. J. BRUCE, *ibid.*, 5 (Trans Tech., Aedermannsdorf, Switzerland, 1985) p. 211.
37. H. HU and J. D. MACKENZIE, *J. Non-Cryst. Solids* **54** (1983) 241.
38. M. ROBINSON, in "Materials Science Forum", 5 (Trans Tech., Aedermannsdorf, Switzerland, 1985) p. 19.
39. C. PHIFER, C. ANGELL, J. P. LAVAL and J. LUCAS, *J. Non-Cryst. Solids* **94** (1987) 315-335.

Received 13 October 1987
and accepted 3 February 1988